Reconciling the working strokes of a single head of skeletal muscle myosin estimated from laser-trap experiments and crystal structures

John Sleep*†, Alexandre Lewalle*, and David Smith‡

*Randall Division, King's College London, SE1 1UL London, United Kingdom; and ‡Department of Physiology, Monash University, Clayton, Victoria 3800, Australia

Edited by Edward D. Korn, National Institutes of Health, Bethesda, MD, and approved December 6, 2005 (received for review July 28, 2005)

Myosin generates force by a rotation of its lever arm. Crystal structures of myosin II indicate an unloaded working stroke of 10–12 nm, a range confirmed by recent x-ray interference experiments. However, when an actin filament, held between two weakly, optically trapped beads is made to interact with a single head of skeletal myosin, the bead displacements have often been reported as having a mean value of 5–6 nm, a value that is commonly interpreted as the working stroke. In general, the observed displacement is not expected to be equal to the working stroke because the kinetics of the stroke is necessarily strain-dependent: this effect biases the frequency of binding events to different actin sites so that displacements smaller than the working stroke are preferentially selected. Our analysis is tailored to current trap experiments, in which the time resolution is insufficient to detect prerigor states. If the preceding transitions are in equilibrium, the mean displacement is zero, contrary to observations in the presence of ATP. However, under ATP-cycling conditions, we find that the mean displacement is deflated to 0.3–0.7 of the true working stroke, depending on the equilibrium constant of the stroke and the rate at which the first myosin product state can detach from actin. The primary working stroke of processive myosin motors as measured by optical trapping is similarly uncertain.

optical | tweezers | molecular motor

The swinging-lever-arm model for muscle contraction is supported by a great variety of experiments, but there are significant disagreements over the size of the swing. All of the current methods suffer from some ambiguity in interpretation; for example, the estimate derived from crystallography is dependent on structures of myosin heads in the absence of actin (1, 2). However, there is reasonable agreement between this estimate and that derived from x-ray interference experiments (3). For the purposes of this work, attention will be focused on whether the difference between the estimates of 10–12 nm based on these methods and the 5- to 6-nm displacement commonly observed for single-headed interactions in optical trap experiments (4–7) can be explained by a reinterpretation of the latter method.

In optical trap experiments, an actin filament is held taut between two weakly trapped beads and is allowed to interact with a single tethered myosin head (Fig. 1). An obvious possibility is that the small step size commonly reported might be due to the myosin either not being attached in an appropriate manner or alternatively not being oriented correctly relative to the actin filament. As will be made evident in the discussion, these possibilities do not stand up well to serious analysis, and we believe that there is a more fundamental error in current methods of deducing the working stroke from optical trap data. At present, the time resolution of bead detection in the three-bead experiment is not adequate to detect the prestroke bound state, which means that an individual working stroke cannot be characterized and that the size of the working stroke can only be estimated on a statistical basis. Binding events are detected by the reduction in variance of bead position (4), which is facilitated by the use of traps, whose stiffness is low relative to that of myosin. Such weak traps allow substantial movement of the bead–actin–bead dumbbell along the axis of the actin filaments

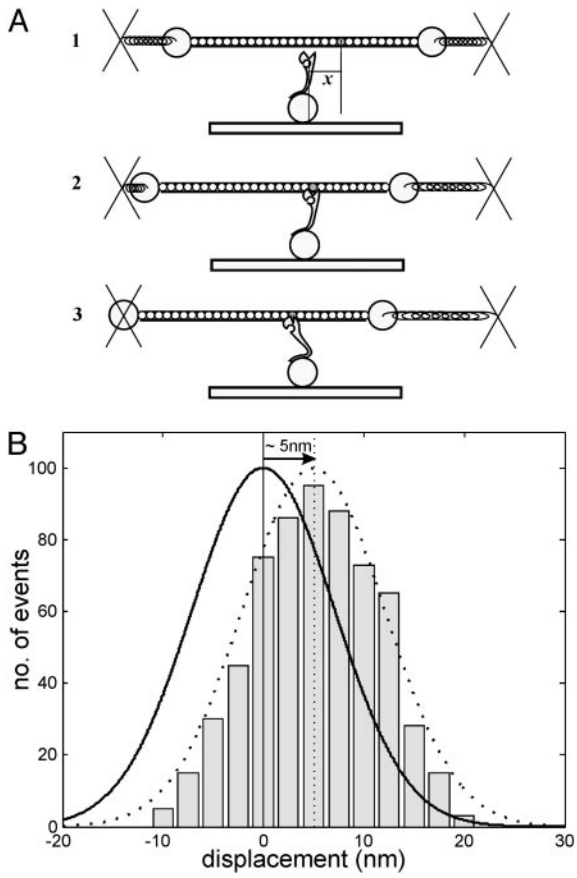

Fig. 1. Displacement of actin–bead dumbbell by a single myosin head. (*A*) Schematic of the three-bead trap experiment with an optically trapped actin filament, showing the myosin free (1), initially bound to actin (2), and after a working stroke (3). (*B*) The frequency of displacements of the free filament is a Gaussian centered on zero, and the histogram shows a typical distribution of displacements with bound myosin, displaced by the effects of the working stroke.

Conflict of interest statement: No conflicts declared.

This paper was submitted directly (Track II) to the PNAS office.

†To whom correspondence should be addressed at: Randall Division, New Hunt's House, Guy's Campus, King's College London, London SE1 1UL, United Kingdom. E-mail: john.sleep@kcl.ac.uk.

www.pnas.org/cgi/doi/10.1073/pnas.0506272103

(SD 10–15 nm), and correspondingly four or five actin monomers are accessible at any time. Molloy and coworkers (4) observed that the positions of the dumbbell while bound to myosin could be described by a Gaussian distribution with the same half-width as that describing the positions of the free dumbbell (see Fig. 1), and they proposed that the displacement in the mean position corresponds to the working stroke. This idea represented a major improvement in interpretation and has gained general acceptance. The equality of the observed displacement and the working stroke is valid if the myosin makes a stroke after every actin-binding event. More generally, the displacement equals the working stroke if the probability of an actin-binding event leading to product release and experimental detection is symmetrical about the mean position of the myosin head. There are fundamental reasons for supposing that in general this condition is not satisfied, because the equilibrium constant of the working stroke must be dependent on elastic strain in the myosin and thus on the initial position of the dumbbell at the time of binding to actin. In the muscle fiber, the experimental consequences of this principle were first demonstrated many years ago (8).

Qualitative Idea

In essence, the Molloy interpretation is equivalent to myosin binding to the actin monomer immediately opposite and undergoing a +5-nm working stroke. We propose instead that the equivalent single event is myosin binding to an actin monomer at −5 nm, undergoing a +10-nm working stroke to again yield the observed displacement of +5 nm. The reason for this expectation is elaborated in Fig. 2, in which the circles represent the positions of the actin monomers before and after the working stroke. The Gaussian curves indicate the probability distributions of the observed pre- and poststroke states. These distributions are the same as those described by Molloy (4), because the distribution of the prestroke state is the same as that of the free dumbbell. Each possible binding site in the poststroke state (A·M) is displaced by the same distance h from its position in the prestroke (A·M·ADP·P_i) state; if the dumbbell position is x in the prestroke state, its position is $x + h$ in the poststroke state.

If the probability of the stroke is symmetrical about the mean position of the myosin head, the mean observed displacement U equals the full working stroke h. However, the work done by the power stroke (and hence its equilibrium constant) is x-dependent, which upsets this symmetry. The more positive the value of x, the more the stroke increases the strain and the more the equilibrium constant for the transition is reduced. The probability of the stroke is therefore less for those values of x that produce more work, which tends to reduce U to a value of $< h$. This effect is illustrated in Fig. 2*B*, where the thickness of the arrows indicates the relative probability of the transition. The monomer located at the center of the poststroke state distributions has been shaded in black in Fig. 2. The Molloy interpretation of trap data assumes implicitly that this monomer is also at the center of the distribution before the stroke (the gray-shaded monomer), which would be true if the stroke probability were symmetrical in x (Fig. 2*A*). In the more likely case of the stroke probability having an asymmetrical x-dependence (Fig. 2*B*), the gray monomer is located to the left of the center of the distribution, i.e., in a less probable location than at the center. However, the smaller likelihood of this prestroke state is compensated by the greater probability of the stroke occurring. The extent to which the observed displacement is reduced relative to the working stroke will be characterized in terms of the deflation factor U/h. Its exact value depends on the detailed mechanism and on the kinetics of the overall crossbridge cycle. The displacement observed in the optical trap should no longer be equated with the working stroke without appropriate justification.

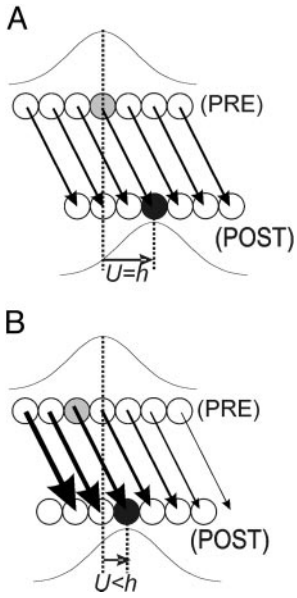

Fig. 2. Schematic of the potential effect of strain dependence on the observed displacement U. The upper and lower rows of circles in *A* (strain-independent transition) and *B* (strain-dependent transition) represent the positions of the actin monomers before and after the working stroke. *A* is in the absence of strain dependence, and *B* is in its presence. Gaussians show the distributions of the dumbbell position before and after the stroke. Vertical lines indicate the center of the distributions to emphasize the magnitude of their displacement U. The slanted arrows show the displacement, by a constant distance h, of individual monomers during the stroke; the line thickness is a measure of the probability of myosin performing the stroke when bound to a particular monomer. (*A*) The distributions are shifted by the same amount as the individual monomers. (*B*) $U < h$ arising from the strain dependence of the stroke probability. The monomer at the center of the poststroke distributions is shaded black, and its location before the stroke is shaded gray. In *A*, the gray site is at the center of the prestroke distribution, whereas in *B* it is offset from the center.

Theory

At present, myosin-binding events are detected with a 5- to 10-ms time resolution and short-lived states that occur before the A·M rigor state are ignored in the present analysis. The working stroke is known to be associated with the release of P_i, and there are muscle-fiber (9–15) and single-myosin experiments (16) that suggest that phosphate is released after the working stroke. We therefore consider the kinetic scheme

$$\underset{p_1}{\text{M·ADP·P}_i} \underset{k_{-1}(x)}{\overset{k_1(x)}{\rightleftharpoons}} \underset{p_2}{\text{AM·ADP·P}_i\text{(pre)}} \underset{k_{-2}(x)}{\overset{k_2(x)}{\rightleftharpoons}} \underset{p_3}{\text{AM·ADP·P}_i\text{(post)}} \underset{k_{-3}}{\overset{k_3}{\rightleftharpoons}} \underset{p_4}{\text{AM}} \overset{g}{\rightarrow}. \qquad [1]$$

Reactions 1, 2, and 3 are binding to actin, the working stroke, and the release of products (P_i and ADP, in that order). The probabilities of occupying the different states are denoted by p_i. In the absence of added P_i, the flux associated with k_{-3} is negligible.

The rates of myosin reactions that involve mechanical movements must be dependent on the longitudinal off-set distances x from myosin to binding sites on the equilibrium position of the detached actin filament. These sites are brought to the myosin by the Brownian forces that drive longitudinal position fluctuations of the dumbbell. After binding, the restoring force of the traps

is balanced by an equal longitudinal force in the myosin molecule when bound. Myosin heads display a stiffness k_m of 1–3 pN/nm in the dumbbell experiment, whereas the trap stiffness κ_t is typically 0.02–0.08 pN/nm, so the strain in myosin is much smaller than the displacement of the dumbbell. If myosin binds to a monomer at position x on the resting dumbbell, and the dumbbell relaxes by a distance u in the opposite direction, the strain energy in the system is $1/2k_m(x - u)^2 + 1/2k_tu^2$. This energy is minimized at equilibrium, where the forces $k_m(x - u)$ and k_tu are equal. The corresponding strain energy is $1/2kx^2$, where k is the stiffness of myosin and the traps acting in series. Because k_t is much smaller than k_m, most of this energy resides in the traps. It is this energy cost that dominates the binding affinity

$$K_1(x) = K_1 \exp(-\tfrac{1}{2}\beta\kappa x^2), \qquad [2]$$

($\beta = 1/k_BT$). Likewise, the equilibrium constant for stroke transition is of the form

$$K_2(x) = K_2 \exp(-\beta\kappa h(x + h/2)), \qquad [3]$$

for a working stroke h, which is modulated by the difference in the elastic energies $1/2\kappa(x + h)^2$ and $1/2\kappa x^2$ of the poststroke and prestroke states. We require the frequency at which the myosin enters state 4, namely

$$J_4(x) = k_3\, p_3(x), \qquad [4]$$

where $p_3(x)$ is the occupation probability of state 3. Following the usual method of analyzing experimental data, the mean displacement U is calculated as the event-weighted average

$$U = \frac{\int (x + h)J_4(x)dx}{\int J_4(x)dx}. \qquad [5]$$

For convenience, the sum over binding sites has been replaced by an integral.

System at Equilibrium. The critical steps of actin-binding and the working stroke are rapid relative to the release of products and may therefore be close to equilibrium even under ATP-hydrolyzing conditions. Evidence for the closeness of the actin-binding step to equilibrium is provided by the approximately hyperbolic dependence of the rate of M·ADP·P_i binding to actin on actin concentration together with the absence of a significant lag phase over the full range of actin concentrations (17). The working stroke is similarly rapid and reversible (8).

In the absence of ATP, the product-release step and the actin-binding and working-stroke transitions all come to equilibrium. Then, $p_3(x) = K_2(x)K_1(x)p_1$, which is proportional to $\exp(-1/2\beta\kappa(x + h)^2)$, a Gaussian centered about zero poststroke strain, because its x-dependence is determined only by the Gibbs energy of the poststroke state. In the present model, it is this population that specifies the event-averaged stroke U through Eqs. **4** and **5**. This equilibrium situation is achieved at concentrations of ATP <10 nM such that $g \ll k_{-3}$ where $k_{-3} \approx 0.05\ s^{-1}$. At the levels of ATP used experimentally (1–10 mM), the observed value of U is not zero, which must result from x-dependent changes in the state populations induced by ATP cycling.

Effects of ATP Cycling. Under steady-state conditions, the net fluxes $k_1(x)p_1(x) - k_{-1}p_2(x)$, $k_2(x)p_2(x) - k_{-2}(x)p_3(x)$, $k_3p_3(x) - k_{-3}p_4(x)$, and $gp_4(x)$ are all equal. Hence

$$\frac{p_3(x)}{p_2(x)} = \frac{k_2(x)}{k_{-2}(x) + g_3}, \quad \frac{p_2(x)}{p_1} = \frac{k_1(x)}{k_{-1} + g_2(x)}, \qquad [6]$$

where $g_3 = k_3g/(k_{-3} + g)$ and $g_2(x) = k_2(x)g_3/(k_{-2}(x) + g_3)$ are effective rate constants for escaping from states 3 and 2 in the forward direction, and the detachment rate k_{-1} is assumed to be x-independent. Note that the equilibrium result is recovered when $g \to 0$.

In the presence of micromolar ATP, $g \gg k_{-3}$ and $g_3 \approx k_3$, which is assumed in what follows. A nonzero mean displacement is achieved because the extent of departures from equilibrium depends on the value of x. Eq. **6** shows that the stroke transition is in equilibrium if $k_3 \ll k_{-2}$, which is approximately satisfied under experimental conditions (see below). However, binding to actin is equilibrated when $g_2(x) \ll k_{-1}$, which is not satisfied except at large positive x where $g_2(x)$ is driven down by the equilibrium constant $K_2(x)$. Thus, steady-state cycling selectively reduces the population of the prestroke state at more-negative values of x, thereby shifting the distribution of events to give a positive mean.

The calculation can be simplified by noting that $p_3(x)/p_1$ can be written in the form $K_2(x)k_1(x)/\{k_{-1} + K_2(x)k_3 + k_{-1}k_3/k_{-2}(x)\}$, which becomes independent of stroke kinetics if the last term in the denominator is small. Thus, the rate of entry to state 4 is

$$J_4(x) \approx k_3 \frac{K_2(x)k_1(x)}{k_{-1} + K_2(x)k_3} p_1, \qquad [7]$$

when $k_3/k_{-2}(x) \ll 1 + K_2(x)k_3/k_{-1}$, a condition that appears to be satisfied experimentally. This approximate result involves only the known strain dependence of the stroke equilibrium constant $K_2(x)$ and requires no knowledge of the stroke rate $k_2(x)$.

Numerical Predictions

For the kinetic scheme of the last section, mean displacements were calculated from Eqs. **5** and **7** using rate constants around the following set of values: $k_{-1} = 1{,}000\ s^{-1}$, $K_2 = 20$, $k_3 = 75\ s^{-1}$, and $k_{-3} = 0.05\ s^{-1}$. The rate k_{-1} of actin dissociation from the prestroke state is estimated from the variation of sinusoidal stiffness with frequency, giving $1{,}000\ s^{-1}$ for cycling myosin at 20°C (18) and $400\ s^{-1}$ for M·ATPγS at 5°C (19). A better analog of the M·ADP·P_i state, namely M·ADP·AlF_4, displays similar characteristics (B. Brenner, personal communication). The value for K_2 is estimated by modeling the rate of the phase-2 length–step response in fibers (14) and is probably in the range 10–40. The stated value of k_3 is limited by the rate of P_i release, which is well characterized from experiments with the phosphate binding protein (17). The rate of stroke reversal k_{-2} is required to verify the inequality under Eq. **7**. Length–step responses in fibers give $k_{-2} \approx 250\ s^{-1}$ for frog muscle at 3°C and rabbit psoas at 20°C (20). As $k_3/k_{-2} = 0.3$, the inequality is well satisfied at negative x and weakly at positive x where $K_2(x) < 1$. The resulting deviations from Eq. **7** depend on the strain-dependent kinetics of the working stroke, and generate errors of order 1–2% in the predicted mean displacement.

Fig. 3 shows the predicted "deflation factor" U/h (mean displacement/working stroke) as a function of trap stiffness κ and the kinetic parameters k_{-1} and K_2. There is also a weak variation with the size of the stroke. In fact, U/h as calculated from Eqs. **4–6** is a function of the three dimensionless parameters $\tilde{h} \equiv (\beta\kappa/2)^{1/2}h$, k_{-1}/k_3, and K_2. With $\kappa = 0.08$ pN/nm, $h =$ 10 nm, and the standard set of kinetic parameters, $U/h = 0.55$, which fortuitously accounts for the 2-fold difference between the working strokes estimated from trap data and crystal structures. Over the range of plausible values of k_{-1} (500–2,000 s^{-1}) and K_2

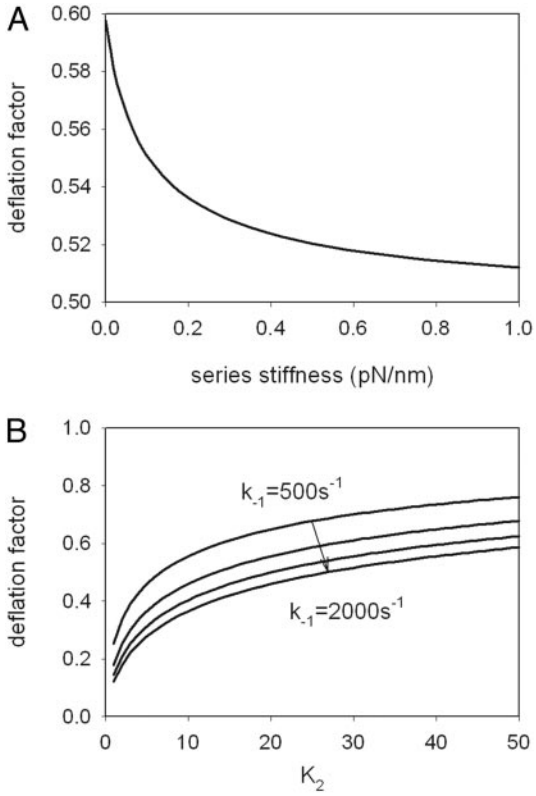

Fig. 3. Mean dumbbell displacement in optical trap experiments as a fraction of the myosin working stroke h (deflation factor). (*A*) Weak variation with myosin-trap stiffness k at $h = 10$ nm. (*B*) Larger variations with respect to the strain-free equilibrium constant K_2 of the stroke, for $k = 0.08$ pN/nm and four values of the prestroke detachment rate k_{-1} in intervals of 500 s^{-1}. *A* can be used for other values of h if the scale of the abscissa is multiplied by $(10/h)^2$. *B* can be used for other values of k_3 because the deflation factor is a function of k_{-1}/k_3; thus, doubling the value of k_3 is equivalent to halving the value of k_{-1}.

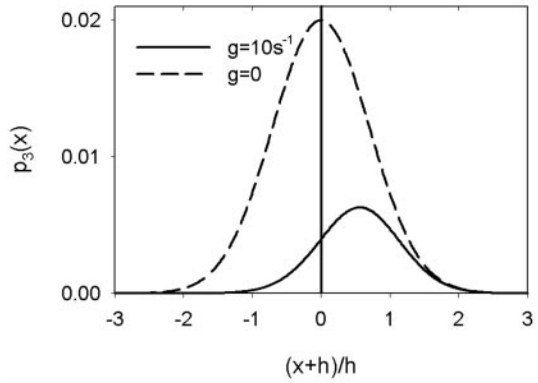

Fig. 4. The frequency of detected poststroke events in the optical trap is proportional to the probability of myosin occupying the A·M·Pr state, here shown as a function of head-site distance x on the resting dumbbell for the four-state model of the main text. The quantity $(x + h)/h$ is the displacement on this site as a fraction of the working stroke h. In the absence of ATP cycling ($g = 0$), the mean displacement is zero. A mean displacement of $0.55h$ is predicted in the presence of 5 mM ATP ($g = 10\ s^{-1}$).

(10–40), the deflation factor varies between 0.37 and 0.74. It is of interest to check which reaction steps produce these results by being out of equilibrium. Because $k_3/k_{-2} = 0.3$, the working-stroke transition remains reasonably close to equilibrium. However, for most binding sites, the binding step stays out of equilibrium because $g_2(x) > k_{-1}$ except at positive values of x where the stroke is energetically unfavorable. The effects of cycling on the state probabilities are shown in Fig. 4.

Discussion

The problem of interpretation of optical trap experiments with skeletal muscle myosin arises because at present the position of the prestroke state cannot be determined. The working stroke cannot be determined from a single interaction but can only be inferred on a statistical basis. Our analysis indicates that the predicted relation between the mean displacement of current trap experiments and the working stroke is model-dependent and that the experimental discrepancy between trap results and crystal structures can be explained readily by a model of the crossbridge cycle in which the phosphate is released after the working stroke.

The P_i release step has a special status in that it is the first step in the scheme that (in the absence of added P_i) is known to be irreversible and thus commits the myosin to releasing ADP and forming A·M, the rigor state that is detected in optical trap experiments. The failure of optical trap experiments to directly measure the working stroke arises from a suspected asymmetry of the flux with respect to strain. The equilibrium constant of the strain-dependent working stroke is the one function that has to be asymmetric. The form of this function does not influence the observed displacement if it comes after a step of commitment. This conclusion can be verified from the existing kinetic model by making step 1 irreversible ($k_{-1} = 0$), in which case $J_4(x) = k_1(x)p_1$ (from Eq. **7**) giving $U = h$ (Eq. **5**). There is a considerable body of evidence from both muscle-fiber experiments (9–15) and single-molecule experiments (16) that favors the working stroke before P_i release.

If this model is appropriate, deflation is greatest when both the actin-binding step and the working stroke are in equilibrium ($k_{-1} \gg K_2(x)k_3$, $k_{-2} \gg k_3$), for in this case zero mean displacement is observed (deflation factor = 0). The solution kinetics of actin binding to M·ADP·P_i unequivocally characterize actin binding as approximating an equilibrium (17). The case for near-equilibrium conditions of the states connected by the working stroke is similarly independent of a detailed kinetic model, because phase-2A tension recovery in the muscle fiber is faster than all subsequent phases, including phosphate release (15).

Although several groups using optical trap have reported a mean displacement (U) of ≈5 nm for single myosin heads interacting with actin, there have also been reports of larger values in slightly different circumstances. Tanaka *et al.* (21) have investigated the interaction of actin with single-headed myosin molecules incorporated into an artificial myosin filament consisting primarily of myosin tails. They report a value for U of ≈10 nm when the actin filament is aligned with the myosin filament, with lesser values for increasing angles between the two filaments. Furthermore, they point out that because of their compliant actin-bead links, the value should probably be corrected up to 15 nm. However, an attempt to confirm these observations failed to reveal either orientation dependence or a large step size (E. Meyhofer and U. Michigan, personal communication). It might be thought that the mode of attachment of the myosin head to the surface was critical for full activity, and indeed myosin-S1 bound directly to a nitrocellulose surface moves actin considerably more slowly than in an unloaded muscle fiber. Yanagida and coworkers (22) solved this problem by attaching the S1 via a biotinylated light chain to a streptavidin-coated surface. However, S1 attached in this manner still gives a displacement of ≈5 nm (23). When bound to a surface the S1 head has been found to rotate relatively freely about its long axis, particularly when bound via a biotinylated light chain, and this

characteristic would be expected to eliminate the significance of orientation on the observed value of U (24). The final argument against orientation being an influence is that estimates of U for different S1 heads (presumably at different orientations) cluster quite closely at ≈5 nm, and values of >7 nm are extremely rare, which is not the behavior expected if the value for a correctly oriented filament is ≈10 nm. A related possibility is that S1 is not bound to the surface in a way that allows it to interact with actin in a fully functional manner. This idea is unlikely to be true because many methods of attachment to the surface have been used, including direct attachment to nitrocellulose, binding via a range of antibodies directed at different parts of the myosin and via biotinylated light chains. All methods have yielded similar results despite binding via biotin giving substantially higher rates in the motility assay (22).

A second circumstance in which larger displacements have been reported is for myosin that has been bound to the surface via an antibody to maximize the chance of both heads being available for interaction. Tyska *et al.* (7) reported a value of 12 nm for dimeric myosin and only 6 nm for myosin-S1. Although this result is illuminating for considering head–head interactions, it is not relevant for the present theory of the action of single-headed myosin. However, for dimeric myosin, it is evident that the second head would have a much-restricted access to actin monomers, which could force the observed working stroke of the second head to be close to its true value.

For several classes of myosin, the overall working stroke has been shown to take place in two steps (25, 26). There are theoretical arguments favoring the existence of a separate small additional working stroke associated with ADP release even for skeletal muscle myosin (27). The theory described in this work is only relevant to the first step, but for those myosin molecules that display two steps, most of the net displacement comes from the first step.

Weak traps have been used for actomyosin experiments primarily to facilitate event detection because they maximize the contrast between the variance of dumbbell position during bound and free periods. A secondary reason was that the weak-trap regime minimized the correction factor $(k_m + \kappa_t)/k_m$ for the stiffness of the traps. It should be noted that reducing the trap stiffness does not help the manifestation of the full working stroke because its effect in reducing the x-dependence of the equilibrium constant $K_2(x)$ is exactly compensated by the increase in the range of x explored by the free dumbbell [controlled by $K_1(x)$].

We have dealt with the existing data that only allows detection of events of >5- to 10-ms duration. The rate of reversal of the working stroke is ≈250 s^{-1} and the rate of P_i release 75 s^{-1}, so that ≈75% of stroke events are followed by a reversal of the working stroke and, having a lifetime of ≈4 ms, go undetected. If these short events could be detected, the deflation factor relating the observed displacement to the working stroke h would be sensitive to the strain-dependence of the stroke rate $k_2(x)$. The potential of such new data will be explored elsewhere.

A uniform distribution of binding sites on F-actin was used for modeling. Provided that, during data collection, the dumbbell is moved in a uniform manner past the myosin filament by an integral number of actin repeats, the actin filament can be treated as uniform with respect to myosin interaction (6).

Optical trapping methods have been particularly successful at elucidating the properties of processive motors such as myosin-V (28, 29). Myosin-V steps by 36 nm, the repeat distance of the actin filament, yet the observed displacement of a single-headed myosin-V is only ≈20 nm. It has been suggested (29) that the step of 36 nm corresponds to working stroke of 20 nm and that the last 16 nm are accounted for by a diffusional search. Although there may be some element of diffusional search in the mechanism, we suggest that the working stroke of single-headed myosin-V may well be significantly more than 20 nm, and the need to postulate a diffusional search may be much reduced.

In principle, the ideas in this work are equally relevant for experiments with other single-headed (kinesin or dynein) motors under circumstances in which several tubulin subunits can be accessed.

This work was supported by the Medical Research Council (U.K.) and National Institutes of Health Grant AR048776.

1. Rayment, I., Holden, H. M., Whittaker, M., Yohn, C. B., Lorenz, M., Holmes, K. C. & Milligan, R. A. (1993) *Science* **261,** 58–65.
2. Houdusse, A., Szent-Gyorgyi, A. G. & Cohen, C. (2000) *Proc. Natl. Acad. Sci. USA* **97,** 11238–11243.
3. Reconditi, M., Linari, M., Lucii, L., Stewart, A., Sun, Y. B., Boesecke, P., Narayanan, T., Fischetti, R. F., Irving, T., Piazzesi, G., *et al.* (2004) *Nature* **428,** 578–581.
4. Molloy, J. E., Burns, J. E., Kendrick-Jones, J., Tregear, R. T. & White, D. C. (1995) *Nature* **378,** 209–212.
5. Ruff, C., Furch, M., Brenner, B., Manstein, D. J. & Meyhofer, E. (2001) *Nat. Struct. Biol* **8,** 226–229.
6. Steffen, W., Smith, D., Simmons, R. & Sleep, J. (2001) *Proc. Natl. Acad. Sci. USA* **98,** 14949–14954.
7. Tyska, M. J., Dupuis, D. E., Guilford, W. H., Patlak, J. B., Waller, G. S., Trybus, K. M., Warshaw, D. M. & Lowey, S. (1999) *Proc. Natl. Acad. Sci. USA* **96,** 4402–4407.
8. Huxley, A. F. & Simmons, R. M. (1971) *Nature* **233,** 533–538.
9. Lund, J., Webb, M. R. & White, D. C. (1987) *J. Biol. Chem.* **262,** 8584–8590.
10. Lund, J., Webb, M. R. & White, D. C. (1988) *J. Biol. Chem.* **263,** 5505–5511.
11. Kawai, M. & Halvorson, H. R. (1991) *Biophys. J.* **59,** 329–342.
12. Dantzig, J. A., Goldman, Y. E., Millar, N. C., Lacktis, J. & Homsher, E. (1992) *J. Physiol.* **451,** 247–278.
13. Ranatunga, K. W., Coupland, M. E. & Mutungi, G. (2002) *J. Physiol.* **542,** 899–910.
14. Smith, D. A. & Sleep, J. (2004) *Biophys. J.* **87,** 442–456.
15. Sleep, J., Irving, M. & Burton, K. (2005) *J. Physiol.* **563,** 671–687.
16. Takagi, Y., Shuman, H. & Goldman, Y. E. (2004) *Philos. Trans. R. Soc. London Ser. B* **359,** 1913–1920.
17. White, H. D., Belknap, B. & Webb, M. R. (1997) *Biochemistry* **36,** 11828–11836.
18. Kawai, M. & Halvorson, H. R. (1989) *Biophys. J.* **55,** 595–603.
19. Kraft, T., Yu, L. C., Kuhn, H. J. & Brenner, B. (1992) *Proc. Natl. Acad. Sci. USA* **89,** 11362–11366.
20. Kawai, M. (1986) *J. Muscle Res. Cell Motil.* **7,** 421–434.
21. Tanaka, H., Ishijima, A., Honda, M., Saito, K. & Yanagida, T. (1998) *Biophys. J.* **75,** 1886–1894.
22. Iwane, A. H., Kitamura, K., Tokunaga, M. & Yanagida, T. (1997) *Biochem. Biophys. Res. Commun.* **230,** 76–80.
23. Steffen, W., Smith, D. & Sleep, J. (2003) *Proc. Natl. Acad. Sci. USA* **100,** 6434–6439.
24. Tyreman, M. (2003) Ph.D. thesis (London University, London).
25. Veigel, C., Coluccio, L. M., Jontes, J. D., Sparrow, J. C., Milligan, R. A. & Molloy, J. E. (1999) *Nature* **398,** 530–533.
26. Whittaker, M., Wilson-Kubalek, E. M., Smith, J. E., Faust, L., Milligan, R. A. & Sweeney, H. L. (1995) *Nature* **378,** 748–751.
27. Smith, D. A. & Geeves, M. A. (1995) *Biophys. J.* **69,** 538–552.
28. Mehta, A. D., Rock, R. S., Rief, M., Spudich, J. A., Mooseker, M. S. & Cheney, R. E. (1999) *Nature* **400,** 590–593.
29. Veigel, C., Wang, F., Bartoo, M. L., Sellers, J. R. & Molloy, J. E. (2002) *Nat. Cell Biol.* **4,** 59–65.